Measurement of the Current Related Damage Rate at -50° C and Consequences on Macropixel Detector Operation in Space Experiments

G. Segneri, C. Brown, J.-D. Carpenter, B. Kuhnle, T. Lauf, G. Lutz, P. Lechner, S. Rummel, L. Strüder, J. Treis and C. Whitford

***Abstract*—An experiment was performed to measure the current related damage rate of silicon soon after a 10 MeV proton irradiation at -50° C, in a condition in which the effect of the leakage current annealing is negligible. This measurement is fundamental to predict the spectroscopic performance of the macropixel detectors which will be mounted on the Simbol-X and BepiColombo space missions. Macropixel detectors consist on matrices of Silicon Drift Detectors with an integrated DEPFET readout node on each pixel and offer an optimal solution when a large pixel area is needed but the noise should be kept at levels allowing X-ray spectroscopy. The most critical aspect of the operation of these detectors, in particular of the one which will be used in the BepiColombo mission, is whether the leakage current increase due to the proton irradiation would still allow the required energy resolution. This leakage current increase cannot be predicted with the available models because, during the whole mission, the sensor will be kept at temperatures below -40° C, and the existing empirical parameterizations are valid only at higher annealing temperatures. A too high leakage current may require, for the first time in a space experiment, an annealing procedure to reduce it.**

The irradiation was performed with diodes at the tandem accelerator of the Meier-Leibnitz Laboratorium in Garching with 10-MeV protons and fluences below 10^{11} protons/cm^2, the important range for the missions. The diodes were cooled at a temperature of -50° C during the experiment and biased and read out with a charge sensitive preamplifier to perform a dosimetry based on proton counting. The leakage current was measured at the end of every exposure, before warming up and replacing the samples. Its time evolution after several steps of annealing at 60° C was then studied in the laboratory to check the agreement with the NIEL hypothesis predictions and thus, to validate the experiment. The experimental setup, the measurements of current induced damage rate at -50° C and its annealing are discussed in detail. The consequences on the Simbol-X and BepiColombo experiments are also examined.

***Index Terms*—Radiation damage, Current related damage rate, Semiconductor Detectors, Active Pixel, Macropixel, DEPFET**

I. Introduction

G. Segneri, P. Lechner and G. Lutz are with PNSensor GmbH, Römerstrße 28, D-80803 München, Germany and with MPI Halbleiterlabor, Otto-Hahn-Ring 6, D-81739 München, Germany (e-mail: Gabriele.Segneri@pnsensor.de)

C. Brown, J.-D. Carpenter and C. Whitford are with Department of Physics and Astronomy, Space research Center, University of Leicester, University Road, Leicester, LEI 7RH, UK

B. Kuhnle, T. Lauf, L. Strüder and J.F. Treis are with MPE für Extraterrestrische Physik, Giessenbachstraße, D-85748 Garching, Germany and with MPI Halbleiterlabor, Otto-Hahn-Ring 6, D-81739 München, Germany

S. Rummel is with MPI für Physik, Föhringer Ring 6, D-80815 München, Germany and with MPI Halbleiterlabor, Otto-Hahn-Ring 6, D-81739 München, Germany

A novel detector concept, the macropixel detector [1], was developed in the Semiconductor Laboratory of the Max Planck Institut. In this type of detector, a pixel is made out of a drift chamber [2] with an integrated Depleted P-channel Field Effect Transistor (DEPFET) [3] readout node at the center of it. The input capacitance of a single channel is determined only by the DEPFET equivalent input capacitance: for a standard XEUS-type DEPFET, like the one integrated in these matrices, it is of the order of 40 fF [4]. This capacitance, which is responsible for the thermal and $1/f$ noise, is independent from the size of the sensitive area, and for this reason, these devices are optimal in applications where the requirements of a large pixel area and a low noise should be combined.

The first macropixel detectors will be used in the Simbol-X [5] and BepiColombo [6] missions. Simbol-X will be an orbiting X-Ray telescope with a 30 m focal length. One of the instruments which will be installed in this satellite is a Low Energy Detector Array (LEDA), which will be used for low-energy photon detection and there will be a macropixel detector in its focal plane. BepiColombo will be a planetary exploration mission to Mercury: in order to perform the X-ray Fluorescence Analysis (XRF) of the Mercury crust and measure its elemental abundance, a dedicated instrument, the Mercury Imaging X-ray Spectrometer (MIXS) was designed. This instrument will be mounted on the Mercury Planet Orbiter (MPO) and it will contain two units, a telescope (MIXS-T) and a collimator (MIXS-C). Both units will have macropixel detectors as focal plane arrays. More details about the focal plane arrays of the LEDA and MIX-S instruments can be found in [7], and the informations which are relevant for this work are summarized in Table I.

One of the most critical aspects of the operation of the MIXS sensors is related to the silicon bulk radiation damage due to the Solar wind's protons during the five years of journey to Mercury and the one or two years of operation in its orbit. A consequence of this exposure will be the leakage current increase and the degradation in the energy resolution. The equivalent proton doses are also reported in Table I for the two missions.

In addition, during the travel and the operation, the sensors will be kept for most of the time at temperatures below -40° C: at these low temperatures, the annealing processes responsible for the leakage current reduction will be inhibited, and in a good approximation, they will not occur at all. The knowledge of the leakage current in these conditions is very important

TABLE I
RELEVANT INFORMATIONS ABOUT THE SIMBOL-X AND BEPICOLOMBO MISSIONS AND THE CORRESPONDING MACROPIXEL SENSORS.

	Simbol-X (LEDA)	BepiColombo (MIXS)
Year of launch	2014	2014
Duration of the mission (years)	5	6 (travel) 1-2 (experiment)
Operating Temperature (° C)	-45	-40
pixel size (μm)	625	300
array dimension (pixels)	128×128	64×64
sensitive area (cm^2)	8×8	1.92×1.92
number of drift rings	6	3
wafer thickness (μm)	450	450
integration time (μs)	128	$128 - 192$
energy range (keV)	$0.5 - 20$	$0.5 - 10$
electronic noise (e$^-$ ENC)	5	< 10
required resolution (eV) (FWHM)	150 (at 6 keV)	200 (at 1 keV)
expected radiation dose (1 MeV n/cm^2) (10 MeV p/cm^2)	1.5×10^9 3.8×10^8	1.1×10^{11} 2.8×10^{10}

in order to predict the expected energy resolution and, if needed, plan possible strategies to achieve the target detector performance. In the Simbol-X experiment, the effect will be less remarkable: the pixel leakage current collection volume will be larger due to the larger pixel area, but the proton dose will be almost two orders of magnitude lower and the devices will be operated at a lower temperature.

In order to predict quantitatively the radiation damage effects, a diode irradiation campaign was performed in Garching at the tandem accelerator of the Maier-Leibnitz-Laboratorium (MLL) of the Technical University and the Ludwig Maximilian University of Munich with 10 MeV protons. Protons fluences between 5×10^9 and 10^{11} protons/cm^2 (2×10^{10} and 3.5×10^{11} 1 MeV equivalent neutrons/cm^2) were delivered. This dose range includes the dose which will be received by the BepiColombo MIXS detectors. The diodes leakage current was measured soon after the exposure to protons and the current related damage rate was then extracted.

This paper is organized as follows: a summary of the necessary formulas about the radiation damage phenomenology is provided in the second section, while the effects on the spectroscopic performance are examined in the third section. In the fourth section, the module assembly and the experimental setup are described. The measurement procedures at the accelerator and in laboratory, as well as the hardness factor computation, are described in the fifth section. The results are shown in the sixth section: the extraction of fluence corrections is first discussed, then the evolution of the damage rate as a function of the annealing time at $60°$ C and its value at $-50°$ C are shown. In the last two sections, the consequences on the missions are examined and concluding remarks are given.

II. DEFINITIONS AND USEFUL FORMULAS

The leakage current increase due to radiation damage is proportional to the fluence according to the relationship:

$$\Delta I_{vol} = \alpha \Phi_{eq}, \tag{1}$$

α being the current relate damage rate, ΔI_{vol} the increase of leakage current normalized at $20°$ C per unit of volume, Φ_{eq} the fluence in 1 MeV equivalent neutrons/cm^2.

Due to its exponential dependence on the temperature, the leakage current is always expressed at the reference temperature of $20°$ C. This normalization is obtained through the relationship:

$$\frac{I(T_1)}{I(T_2)} = \left(\frac{T_1}{T_2}\right)^2 \exp\left[-\frac{E_g}{2k_B}\left(\frac{1}{T_1} - \frac{1}{T_2}\right)\right], \tag{2}$$

where $I(T_1)$ and $I(T_2)$ are the leakage currents measured at the temperatures T_1 and T_2, E_g is the energy gap in the Silicon ($E_g = 1.11$ eV) and k_B the Boltzmann constant.

The fluence normalization to 1 MeV equivalent neutrons is performed assuming the non-ionizing energy loss (NIEL) scaling hypothesis, according to which, the induced displacement damage scales linearly with the non ionizing energy loss in the material [8]. The fluence $\Phi_p(E)$, related to an irradiation with particles of a type p and an energy E, is proportional to the 1 MeV neutron fluence equivalent Φ_{eq} through an hardness factor κ:

$$\Phi_p(E) = \kappa \Phi_{eq}, \tag{3}$$

where

$$\kappa = \frac{D_p(E)}{D_n(1\text{ MeV})}, \tag{4}$$

and $D_p(E)$ and $D_n(1\text{ MeV})$ are the induced displacement damage (defined in [8]) for a given proton with an energy E and a 1 MeV neutron. The hardness factor used in these studies are tabulated in [9].

A decrease with time of the current related damage rate is due to the annealing of various defects with different time constants, contributing to the total current. Its temporal behaviour is expressed in the following empirical parameterization:

$$\alpha(t) = \alpha_I \; exp\left(-\frac{t}{\tau_I}\right) + \alpha_0 - \beta \log(t/t_0), \tag{5}$$

where the constants values and their dependence on the annealing temperature are reported in [10]. The current related damage rate observed after 80 minutes of annealing at $60°$ C is always quoted as a reference value and the average obtained by the RD 48 collaboration is $(3.99 \pm 0.03) \times 10^{-17}$ A/cm. The parameterization of Eq. 5 is valid at annealing temperatures higher than $21°$ C and, although alternative expressions are also available, none of them applies to temperature as low as $-50°$ C.

The time constant τ_I of Eq. 5 depends the annealing temperature T_a according to the relation:

$$\frac{1}{\tau_I} = k_{0I} \times \exp\left(-\frac{E_I}{k_B T_a}\right), \tag{6}$$

where $E_I = 1.11 \pm 0.05$ eV and $k_{0I} = 1.2^{+5.3}_{-1} \times 10^{13}$ s^{-1}. As an example, according to this formula, the speed of annealing at $-40°$ C is 10^6 times slower than at $21°$ C.

III. Energy resolution

The energy resolution of an X-ray spectroscopic detector can be expressed by the formula:

$$\Delta E = 2.355 \sqrt{\sigma_{Fano}^2 + \sigma_{el}^2 + \sigma_{shot}^2}, \quad (7)$$

where σ_{Fano} is the Fano noise, σ_{el} is the noise due to the readout electronics, σ_{shot} is the shot noise due to the detector leakage current and 2.355 is a conversion factor obtain the Full Width at Half Maximum (FWHM) of a gaussian distribution starting from its variance σ. The noise terms are defined by the relationships:

$$\sigma_{Fano} = \sqrt{w\ F\ E_X}, \quad \sigma_{el} = w\ \sigma_{ENC}, \quad (8)$$

$$\sigma_{shot} = w\ \sqrt{\frac{i_{leak}\ t_{int}}{e}}, \quad (9)$$

where $w = 3.36$ eV is the energy required to create an electron-hole pair, $F = 0.12$ is the Fano factor, E_X is the photon energy, σ_{ENC} is the equivalent noise charge in electrons, i_{leak} is the leakage current, e the electron charge and t_{int} is the integration time. In these macropixel devices, the signals of the pixels of the same row are processed in parallel and the whole matrices is read out in a rolling shutter mode, i.e. the information of a given pixel is processed again only after the whole column is read out. Therefore, the integration time is determined by the sum of the times needed to readout all other pixels of the same column. The foreseen integration times of the Simbol-X and BepiColombo detectors are reported in Table I.

Combining Eq.1 with Eq.7, and using the data of Table I, it is possible to extract the maximum current related damage rate allowing the target resolution. This value is shown in Fig. 1 for the two missions as a function of the operating temperature.

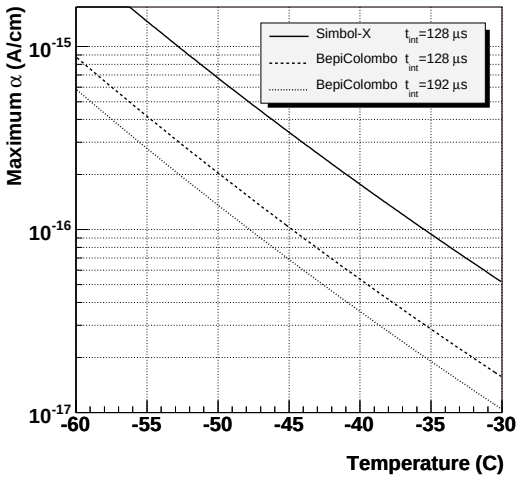

Fig. 1. Maximum current related damage rate allowing the target energy resolution for the Simbol-X and BepiColombo missions as a function of the operating temperature. The integration time (t_{int}) related to the curves is reported.

For the BepiColombo mission, the maximum allowed current related damage rate at an operating temperature of $-40°$ C are 5.4×10^{-17} A/cm and 3.6×10^{-17} A/cm for integration times of 128 μs and 192 μs respectively, which are already smaller than values already measured at room temperature before the annealing cycles (of the order of 9.5×10^{-17} A/cm [10]). This is already a hint that some actions need to be taken, but in order to have a quantify the effect, the results of this experiment are important. A shorter integration time or lower operating temperature would be a solution, but the modification of these parameters is not straightforward due to the implications on the overall spacecraft and electronics design. An annealing procedure would be in this case the most convenient solution.

In the Simbol-X case, the maximum current related damage rate at an operation temperature of $-45°$ C is 3.4×10^{-16} A/cm, and it is more than three times higher than the available measurements with room temperature annealing. However, in order to demonstrate the feasibility of the experiment, it is still necessary to prove that the contribution of defects which would not anneal at $-45°$ C is not remarkable. For this purpose, the the measurement of this work is fundamental.

IV. Experimental Setup

A. Accelerator facility

As already mentioned, this diodes irradiation was performed at the tandem accelerator of the MLL facility. The main advantage of this accelerator is the availability of a 10 MeV proton beam with an energy spread of the order of 2 keV. A monochromatic beam is crucial at these energies since the hardness factor κ has a remarkable dependence on the proton energy. Another important feature of this facility is the possibility to perform irradiation with a relatively low proton rate, which allow a very precisely control of the dose. The parameters of the accelerator were tuned to achieve a beam spread illuminating as uniformly as possible the die, and with a proton rate below $1 - 1.5$ MHz, which allowed a proton counting based dosimetry.

B. Test diodes

Diodes were obtained from three different 450 μm thick wafers produced in the Semiconductor Laboratory of the Max Planck Institut in Munich, with the same technology used in the Simbol-X and BepiColombo matrices. Diodes were available in 10×10 mm^2 dies, each one including three 3.2×3.2 mm^2 squared diodes with guard ring and a squared capacitor, which was not used in these studies. An n^+ ring was also implanted around the die to provide the common bias voltage to deplete the bulk. Each diode was characterized before irradiation. Current-voltage characteristics were measured up to a bias voltage of 200 V. When the guard ring was connected to ground, the leakage current was below 50 pA at a temperature of 21° C, with no hints of breakdown. For these wafers, the pre-irradiation depletion voltage was of the order of $120 - 130$ V.

C. Module assembly

Every die was mounted in a module in order to allow thermal control and biasing and handling during irradiation

and annealing tests. A picture of a module is shown in Fig. 2.

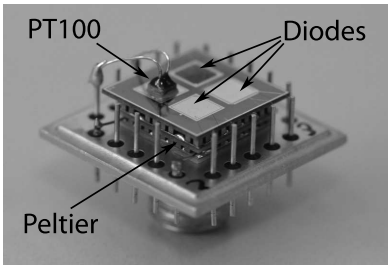

Fig. 2. Picture of a diode module. The main components are also indicated.

Each module was assembled on a squared 20×20 mm^2 gold-plated mechanical support. At the center of the structure, a Peltier module was glued from its warm side. The back side of the die was glued on the top of the cold side of the Peltier. In order to provide the electrical connections with the diodes contacts, five metallic rods were foreseen at each of the four sides of the module (for a total of 20) and perpendicularly to the module's surface. One of the extremities of these rods was micro-bonded to the contacts of the die. The support had also a gold-plated screw on the side opposite to the die in order to connect mechanically and thermally the whole module to a cold finger.

The Peltier module was of a 2-stages type, allowing a maximum temperature difference of 50° C with a 1.3 A current. A PT100 module was glued on the top of the capacitor in order to monitor the temperature of the diodes. The two terminals of the Peltier module as well as the four terminals of the PT100 were also connected via the gold-plated metallic rods.

D. System assembly and environmental control

In order to place the diodes along the beamline, a 60 cm long cylindric vacuum chamber was designed. A scheme of it is shown in Fig. 3, while a view of the experimental area with the setup installed is shown Fig. 4.

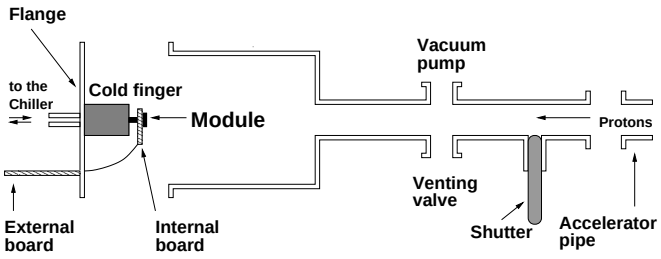

Fig. 3. Scheme of the vacuum cylinder and the flange.

On one side, the cylinder was interfaced with the main vacuum pipe. A manual shutter was placed along the cylinder in order to decouple it from the main pipe and allow the opening of it to replace the modules. Additional openings were introduced for vacuum pumping and venting. On the opposite side, the cylindrical chamber was closed with a flange. The module was

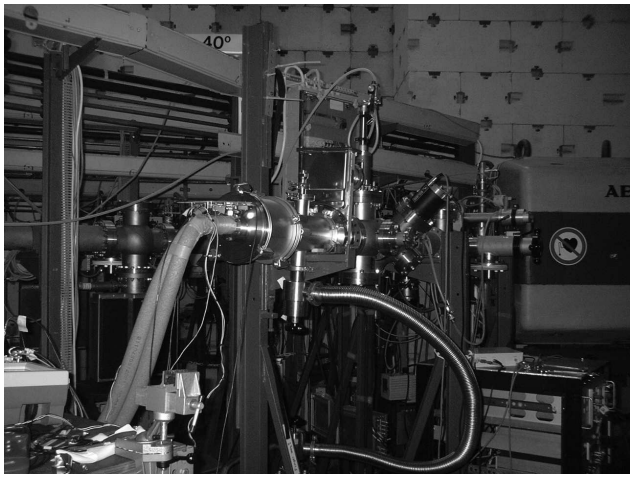

Fig. 4. A view of the experimental area as it was during the experiment. The cylinder was connected to the the accelerator vacuum pipe and the electronics, cooling and vacuum pump are inserted.

screwed on a cold finger attached to the flange. The cold finger was cooled with an external chiller in order to keep the warm side of the Peltier at a constant temperature of 0° C during the operation.

The modules rods extremities which were not bonded to the die, were connected to an internal board. A hole on this board allowed to screw the module on the cold-finger. A Sub-D feedthrough was located on the flange: the connections between the feedthrough and the internal board were achieved with coaxial cables, while externally, a second board was plugged onto the flange.

The preamplification circuits, sketched in Fig. 5, were included in this external board. The same board could also be used to measure the leakage current at the end of every exposition: by moving a jumper of this board, it was possible to disconnect the p+ contact of a diode from its preamplifier, ground it through the a Keithley 487 picoamperemeter (also shown in Fig. 5) and measure the leakage current for every diode without opening the chamber.

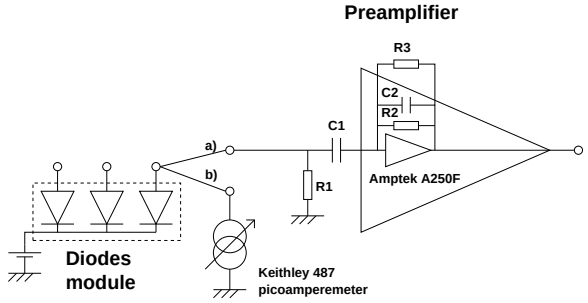

Fig. 5. Scheme of the biasing and preamplifying circuit. When the p+ contact of a diode is connected to the amplification chain according to the modality a) in the figure, the proton counting dosimetry can be performed, while when it is connected to the picoamperemeter in the modality b), the leakage current can be measured.

E. Readout System

A scheme of the overall system used to perform dosimetry is shown in Fig. 6.

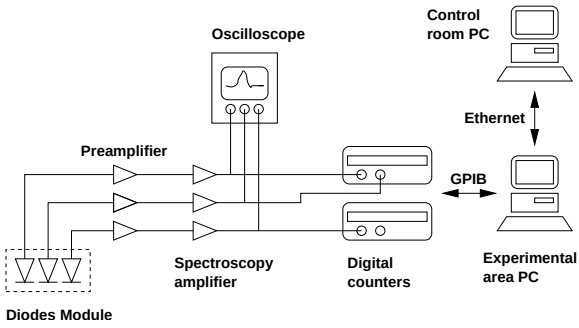

Fig. 6. Scheme of the DAQ system used for dosimetry.

The diodes were depleted during the irradiation applying a positive bias voltage of 150 V to the common n+ contact. The diodes guard rings were directly grounded and each diodes p+ contact was biased to ground potential through 100 MΩ resistors (R1 in Fig. 5) and connected to the charge-sensitive preamplifier. The Amptek A250F circuits were used in this preamplification stage. An additional amplification stage was performed using an ORTEC model 450 spectroscopy amplifier to provide further amplification and reduce the noise through an RC-CR shaper included in the same ORTEC module. At the end of the chain, the overall duration of the pulses was of the order of 300 ns. A precise measurement of the dead time is described in subsection VI-A.

In order to measure the proton rate, two individual two-channels HP53131A digital counters were used. The thresholds were chosen in order to suppress the dark rate without affecting the measured proton rate. The dark rate due to pick-up, measured closing the shutter, was of the order of 20 Hz, negligible with respect to the proton rates during the irradiation (between 200 kHz and 1 MHz).

The digital counters were connected through GPIB with a PC and controlled by a software interface. Through a remote ethernet connection, it was possible from the control room to start and stop the proton counting in correspondence of the opening and closing of a beam shutter placed upstream the beamline. The proton counts were read serially for the three channel and, after every cycle, the three values were stored in a file, together with the updated value of the total number of protons. It was possible to monitor this number online and stop the main beam shutter as soon as the target dose was achieved.

V. Experimental procedures

A. Irradiation

The irradiation campaign took place in November 2007 between the 26^{th} and the 28^{th}. The first day was dedicated to the mounting and commissioning of the system.

A test diode of the same type of the ones used in the irradiation was used to test the setup and adjust the beam positioning. The width of the beam spot on target was of the order of 8×14 mm^2. The beam intensity was also adjusted in order to achieve the target doses with a reasonable exposure duration. The temperature was stable at around -50° C during the irradiation.

As soon as the exposure finished, the leakage current was measured and the module replaced with another one. Irradiated modules were stored in a fridge with -15° C until the end of the irradiation and then stored at -30° C until the annealing behavior was not studied.

B. Annealing

The annealing behaviour was studied in the Semiconductor Laboratory of the Max Planck Institut in Munich. Annealing steps were performed at a nominal 60° C inside an oven. The temperature has been monitored with the PT100 temperature sensors in all the phases of the experiment in order to normalize the time interval to a reference temperature (60° C) through Eq. 6. The diodes were fully characterized at temperatures between 22° C and 25° C at the end of each annealing cycle.

C. Computation of the hardness factor

At a proton energy of 10 MeV, the protons range in silicon is 700 μm, which is larger but comparable with the sensors thickness. After having crossed the whole sensor thickness, the final energy of the protons is around 5.5 MeV and the increase of the induced displaced damage as a function of the depth is remarkable in this energy range.

The effective hardness factor of 10 MeV protons through a 450μm thick silicon layer was computed with the formula:

$$\kappa = \frac{1}{L\ D_n(1\ MeV)} \int_0^L D_p[E(s)]ds, \qquad (10)$$

where ds is an infinitesimal segment of the trajectory of the particle in the material, $E(s)$ is the particle kinetic energy in that segment, $D_p[E(s)]$ the corresponding proton induced displacement damage, and L the total track length.

In order to evaluate the hardness factor numerically, a simulation with GEANT4[11] (version 4.9.1) was performed: protons were generated with a 10 MeV energy and an initial direction perpendicular to the silicon and at each i^{th} track propagation step of length Δs_i, the corresponding induced displaced damage $D_p(E_i)$ was obtained interpolating the values tabulated in [9]. The integral of Eq. 10 was finally replaced by a discrete sum over the number of steps N_{steps}:

$$\kappa = \frac{1}{L} \sum_{i=0}^{N_{steps}} \frac{D_p(E_i)}{D_n(1\ MeV)} \Delta s_i. \qquad (11)$$

According to this method, the volume correction factor and the hardness factor are: $\kappa/\kappa_0 = 1.25 \pm 0.009$, $\kappa = 4.84 \pm 0.03$, where $\kappa_0 = 3.871$ is the hardness factor in an infinitesimally thin layer approximation.

VI. Results

A. Dead time measurement and fluence correction

A precise measurement of the fluence is mandatory in order to extract the current related damage rate. Since the proton counting system used in this experiment has a paralizable behaviour, the dependence of the average measured proton

rate (R_{meas}) on the corresponding true rate (R_{true}), in the presence of a pulse-width imposed dead time τ, is expressed by the relation [12]:

$$R_{meas} = R_{true}\ \exp\left(-R_{true} \times \tau\right). \qquad (12)$$

This function is linear for rates much smaller than $1/\tau$, has a maximum at $R_{true} = 1/\tau$, and $R_{meas}(1/\tau) = 1/(e\tau)$ corresponds to the saturation rate. Once the dead time is known, the formula can be inverted in order to extract numerically the true rate corresponding to the measured one.
It is possible to extract both the dead time that the damage constant from the same fit. According to Eq. 1, the leakage current per unit of volume is related to the true proton flux through the relationship:

$$\Delta I_{vol} = \alpha \Phi_{eq,true} = \alpha\kappa\Phi_{p,true}, \qquad (13)$$

where $\Phi_{eq,true}$ is the true fluence expressed in 1 MeV equivalent neutrons/cm^2, $\Phi_{p,true}$ is the fluence of 10 MeV protons/cm^2 and κ is the already defined hardness factor. From Eq. 1, Eq. 13 and the definition of rate, R_{true} can related to the absolute diode leakage current i_D through the relationship:

$$R_{true} = \frac{\Phi_{p,true}\ S}{t_{irr}} = \frac{\Delta I_{vol}\ S}{\alpha\kappa t_{irr}} = \frac{1}{\alpha\kappa\delta}\left(\frac{i_D}{t_{irr}}\right), \qquad (14)$$

where S is the diode surface, t_{irr} is the duration of the irradiation and δ is the thickness of the diode. According to this equations, the measured proton rate can be related to i_D/t_{irr} according to the relationship:

$$R_{meas} = \frac{1}{\kappa\delta}\ \frac{1}{\alpha}\ \left(\frac{i_D}{t_{irr}}\right)\ \exp\left[-\frac{1}{\kappa\delta}\frac{\tau}{\alpha}\left(\frac{i_D}{t_{irr}}\right)\right]. \qquad (15)$$

In this equation, R_{meas} is a function of i_D/t_{irr}, κ and δ being constants and $1/\alpha$ and τ/α (and thus α and τ) the unknown parameters of the function. The uncorrected measured rate for the diodes used in the annealing studies is shown in Fig. 7 as a function of the i_D/t_{irr} after 80 minutes of annealing at $60°$ C. A fit was performed to extract α and τ and the curve which was obtained is superimposed in the figure. At measured rates below 0.5 MHz, its dependence on i_D/t_{irr} is quasi-linear, while at higher rates the non linearity becomes remarkable and a hint of saturation is visible is visible above 1 MHz. The dead time measured according to this method is (320 ± 15) ns.

B. Damage constant dependence on the annealing time

According to the fit of R_{meas} with respect to i_D/t_{irr}, the value of the damage constant after 80 minutes at $60°$ C is:

$$\alpha = (3.66 \pm 0.05) \times 10^{-17}\ \text{A/cm}. \qquad (16)$$

This value is 1.4 standard deviations below the RD 48 average of $(3.99 \pm 0.03) \times 10^{-17}$ A/cm, having a sigma level of 0.24×10^{-17} A/cm [10]: such a disagreement is not remarkable enough to invalidate the experiment. The dependence of the damage rate on the annealing time at $60°$ C is shown in Fig. 8: with approximately 180 minutes of annealing at this temperature, it was possible to achieve a damage rate as low as 3.1×10^{-17} A/cm.

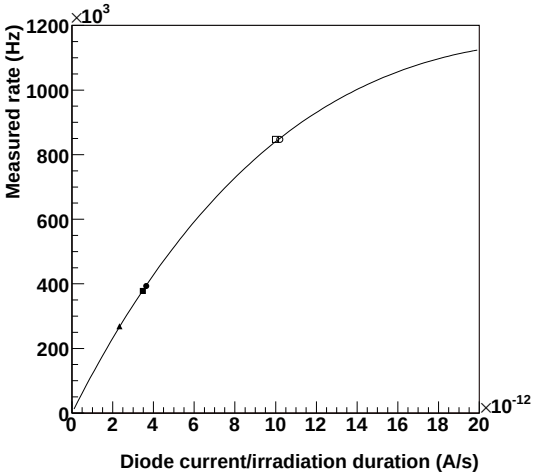

Fig. 7. Measured proton rate without corrections as a function of the ratio between diode leakage current and irradiations duration (i_D/t_{irr}). The experimental measurements are superimposed to the fit with the function of Eq. 15.

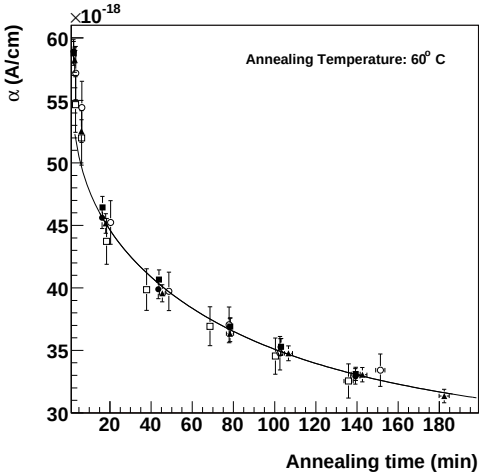

Fig. 8. Damage rate as a function of the annealing time at performed at $60°$ C.

C. Damage constant measurement at $-50°$ C

The diode current measured at $-50°$ C, and normalized to $20°$ C, is shown in Fig. 9 as a function of the corrected fluence. A linear fit was performed and, after dividing the slope by the diode volume, the corresponding damage rate obtained is:

$$\alpha = (11.1 \pm 0.2) \times 10^{-17}\ \text{A/cm}. \qquad (17)$$

The average annealing time at $-50°$ C before the current measurement was 5800 s (~ 100 min) and it was mainly due to the irradiation duration. The damage constant prediction from the Eq. 5 extrapolation is $(11.58 \pm 2) \times 10^{-17}$ A/cm, and it is compatible within one standard deviation with the value obtained in this experiment. This agreement suggests the absence or irrelevance of very fast annealing defects which would be present at $-50°$ C and to which the already existing measurements would have been insensitive.

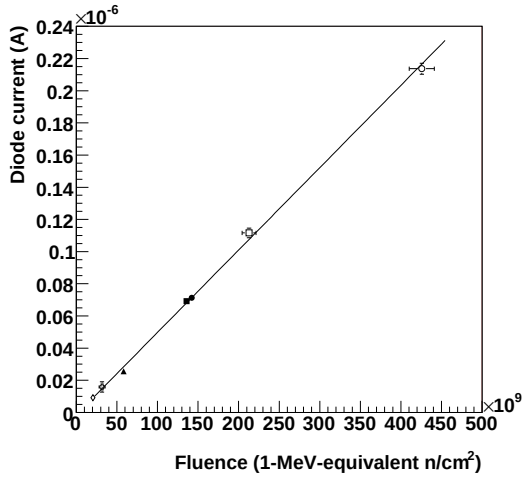

Fig. 9. The diode current measured at $-50°$ C (and normalized at $20°$ C) as a function of the corrected fluence expressed in $1\ MeV$ equivalent neutrons/cm^2. The fit is superimposed to the experimental measurement.

VII. Consequences for the Missions

According to the results shown in this paper, an annealing procedure would be mandatory in the BepiColombo mission in order to achieve the target resolution at an operation temperature of $-40°$ C, and with an integration time not shorter than 128μs. The required annealing time needed was computed inverting Eq. 5 (with the parameters values computed according to the annealing temperature) and it is shown in Fig. 10 as a function of the annealing temperature. Different scenarios are possible according to the highest available annealing temperature: for example, with an annealing temperature of $60°$ C, the required annealing duration would be of 9 minutes. With a duration of the annealing procedure longer than the minimal required, arbitrary safety margins can be obtained. This computation was also repeated for an integration time of $192\ \mu$s: the target resolution can still be achieved and the corresponding minimal annealing duration needed with a temperature of $60°$ C would be of 151 minutes.

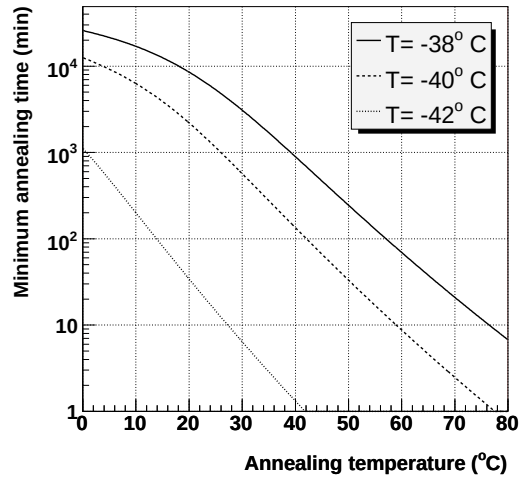

Fig. 10. Minimum annealing time required at different operation temperatures as a function of the temperature of annealing and at an integration time of $128\ \mu$s.

As predicted by the model of Section III, the target Simbol-X resolution can be obtained also with the irradiated sensor, since the measured damage rate at $T_{ann} = -50°$ C obtained from these studies is a factor six smaller than the maximum allowed one at this temperature (6.7×10^{-16} A/cm, from Fig. 1).

VIII. Conclusion

An experiment to measure the current related damage rate in the BepiColombo an Simbol-X operation conditions was successfully completed. The values obtained after 80 minutes of annealing at $60°$ C and at $-50°$ C without annealing are summarized in Table II, together with the relative measurement and prediction from the RD 48 collaboration. The agreement with this model suggests the absence of new low temperature effects which would complicate the detector operation.

TABLE II
Summary of the current related damage rate obtained with this experiment. For comparison, the measurement of the RD 48 collaboration are shown.

annealing conditions	80 min at $60°$ C $\times 10^{-17}$ A/cm	~ 100 min at $-50°$ C $\times 10^{-17}$ A/cm
RD 48	3.99 ± 0.03	11.58 ± 2 (extrapolated)
this experiment	3.66 ± 0.05	11.1 ± 0.2

These results provide very important hints to define the experimental procedures to operate the instruments. In particular, the most important consequence of this measurement is that it will still be possible to achieve the required Simbol-X energy resolution at the project temperature and integration time. In the BepiColombo experiment, annealing will be required to achieve the target resolution.
In order to obtain a more complete insight of the detector performance, matrices, electronics components and modules will be irradiated in the next future.

Acknowledgment

We are grateful to Ludwig Beck and Walter Carli from the Meier-Leibnitz-Laboratorium for the collaboration during the preparation of the measurements and the assistance during the irradiation.

References

[1] C. Zhang et al., "Development of X-type DEPFET Macropixel detectors", *Nucl. Instr. and Meth.* A588, pp. 389-396, 2008
[2] E. Gatti and P. Rehak, "Semiconductor drift chambers - an application of a novel charge transport scheme", *Nucl. Instr. and Meth.* A225, pp. 129-141, 1984
[3] J. Kemmer and G. Lutz, "New semiconductor detector concepts", *Nucl. Instr. and Meth.* A253, pp. 356-367, 1987
[4] M. Porro et al, "Spectroscopic performances of DePMOS detector/amplifier device with respect to different filtering techniques and operating conditions", *IEEE-TNS* vol.53, No.1(2) pp. 401-408, 2006
[5] P. Ferrando et al, "Simbol-X, a new generation hard X-ray telescope", *Proc. SPIE* vol.5168, no.1, pp. 65-76, 2004
[6] R. Grard, M. Navarra and G. Scoon, "BepiColombo - A Multidisciplinary Mission to a Hot Planet", *ESA Bulletin*, vol. 103, pp. 11-19, 2000
[7] J. Treis et al, "DEPFET based Focal Plane Instrumentation for X-Ray Imaging Spectroscopy in Space", *IEEE NSS Conference Record*, N47-3, 2007

[8] A. Vasiliescu, “The NIEL scaling hypothesis applied to neutron spectra of irradiation facilities in the ATLAS and CMS SCT” ROSE/TN/97-2
[9] A.Vasiliescu and G.Lindström, “Displacement damage in silicon”, on-line compilation
[10] M. Moll, “Radiation Damage in Silicon Particle Detectors”, Ph.D. Thesis (Hamburg University), DESY-THESIS-1999-040
[11] S. Agostinelli et al,“GEANT4 - a simulation toolkit”, *Nucl. Instr. and Meth.* A506, pp. 250-303, 2003
[12] W.R. Leo, “Techniques for Nuclear and Particle Physics Experiments”, Second Revised Edition, Springer-Verlag